EGYPTIAN DENTAL JOURNAL
www.eda-egypt.org
VOL. 71, 2145:2154, JULY, 2025
PRINT ISSN 0070-9484 • ONLINE ISSN 2090-2360
ORAL MEDICINE, X-RAY, ORAL BIOLOGY AND ORAL PATHOLOGY
Submit Date : 13-02-2025 • Accept Date : 31-03-2025 • Available online: 10-07-2025 • DOI : 10.21608/edj.2025.359814.3384

NANOGRAPHENE AND CURCUMIN TO IMPROVE THE BIOCOMPATIBILITY OF POLYMETHYL METHACRYLATE (PMMA)

Inas Helwa*; Randa H Mokhtar*; Nermeen S Afifi** *and* Lamis A Hussein ***

ABSTRACT

Graphene-based nanomaterials have outstanding physicochemical and anti-bacterial properties. Curcumin (CUR) is a natural polyphenolic with anti-inflammatory properties. Resin-based materials such as poly-methyl methacrylate resins (PMMA) are widely used in dentistry especially as denture bases, orthodontic brackets and temporary crowns. Despite their extensive uses in the dental field, they still have limitations such as producing mild mucosal irritation and promoting fungal growth. Incorporating nanoparticles such as graphene oxide (nGO) and/or curcumin (nCUR) with PMMA can improve its biocompatibility and reduce inflammation.

The aim of this study was to investigate the in vivo biocompatibility of incorporating nanoparticles of GO or CUR into PMMA. Biocompatibility was evaluated by subcutaneous implantation of the material for 1 week in Wistar rats.

This study included 24 Wistar rats divided into 4 groups; group 1 (Sham group), group 2 (PMMA only), group 3 (PMMA with nGO) and group 4 (PMMA with nGO and nCUR). One-week post-surgical, hematological parameters were assessed. After sacrifice, histological examination was performed to evaluate the thickness of granulation tissue and inflammatory cells count. The data showed normal hematological profile and lower signs of inflammation in samples of PMMA with nGO as compared to the PMMA alone or the PMMA with added nGO and nCUR. In conclusion, adding nGO particles significantly improved the biocompatibility of PMMA as compared to both PMMA alone and PMMA with nCUR.

KEYWORDS: Polymethylmethacrylate, Graphene oxide nanoparticles, Curcumin, Biocompatibility

* Lecturer of Oral Biology, Department of Histopathology, Faculty of Oral and Dental Medicine, Misr International University, Cairo, Egypt
** Associate Professor of Oral Pathology, Faculty of Dentistry, Ain Shams University, Cairo, Egypt
*** Associate Professor of Dental Biomaterials, Department of Prosthodontics and Biomaterials, Faculty of Oral and Dental Medicine, Misr International University, Cairo, Egypt

Article is licensed under a Creative Commons Attribution 4.0 International License

INTRODUCTION

The incorporation of nanoparticles in dental materials offers multiple potentials to improve their physical, chemical and biological properties. The use of nanomaterials improves the biocompatibility, bactericidal effect, tissue response and mechanical properties of various materials. [1] Addition of nanoparticles to dental composites helps improve the aesthetic and mechanical properties of dental composite resin. [2] Graphene is a promising nanomaterial with a hexagonal honeycomb structure made of a single layer of carbon atoms. [3,4] Nanographene Oxide (nGO) has been previously shown to induce proliferation, cell adhesion and differentiation. It can also induce osteogenic differentiation and shows excellent antibacterial properties and hence has been previously used as a scaffold in bone tissue regeneration. [5–10]

On the other hand, the biocompatibility of graphene and its derivatives is debatable. A previous study performed on red blood cells (RBCs) has shown that treatment with nGO led to altered RBCs morphology and hemolysis. [11,12] Another study has shown that high concentrations of nGO can induce loss of cell viability and increased oxidative stress in a lung cancer cell line A549. [13] Similarly, nGO induced a concentration-dependent increase of ROS production in HaCaT skin keratinocytes after 24 h exposure. [14] On the contrary, nGO showed no cytotoxic effects in murine lung epithelial cells FE1 at relatively high doses (5-200 μg/ml). [15] It has been previously shown that Au-deposited GO nanocomposites improved cell viability of mesenchymal stem cells in vitro and lowered their immune stimulation in vivo. The nanocomposites also exhibited anti-oxidative capacity, improved angiogenesis and inhibited cytokines production. [16,17]

Polymethyl methacrylate (PMMA) is a highly biocompatible material that is extensively used in dentistry. PMMA are used mainly for denture bases and orthodontic appliances. [18] Despite its usefulness in multiple dental applications, PMMA promotes the growth of microbes on its surface especially in the oral environment. The addition of nanoparticles with antimicrobial properties (such as nGO) to PMMA is an emerging strategy to improve its longevity and reduce its hazards on oral health.

Curcumin (CUR) is a polyphenolic constituent derived from turmeric. CUR alone is an effective anti-microbial agent; however, it is poorly soluble in water and is cytotoxic in high concentrations. It has been previously shown that the synergistic effect of curcumin loaded graphene oxide (GOCUR) yields potent antibacterial properties.

To address the innovative strategy of incorporating nGO alone and nGO with curcumin (nGOCUR) into PMMA and examine its biocompatibility, we prepared nGO loaded-PMMA as well as nGOCUR-PMMA samples. A rat model was used to examine the tissue response *to* this modified PMMA after 7 days of subcutaneous surgical insertion. The systemic and local tissue response to the material have been evaluated by hematology and histopathology of the surrounding tissue.

MATERIALS AND METHODS

A total of 24 polymethyl methacrylate (PMMA) samples were prepared for subcutaneous surgical insertion. PMMA was prepared from powder and methyl methacrylate monomer (MMA) according to the manufacturer's instructions (Acrostone, Egypt) and as previously described. [19,20] In brief, the molds were made from aluminum alloy with cavities with the dimensions of 65 mm (length) ×10 mm (width) ×2.5 mm (depth). The powder in each group was mixed with the liquid monomer according to manufacturers' instructions, mixing was continued until a consistent mixture was obtained. When the mixture reached the dough stage it was packed inside the molds. Before pouring the mixture into the mold a separating medium of sodium alginate was applied to the mold for easy separation. The acrylic resin was left to set completely and then removed

from the mold. The set acrylic was further cut into smaller samples (5 mm length X 5 mm width X 2.5 mm depth) to be suitable for surgical insertion. Graphene oxide nanosheets (nGO) and curcumin-loaded graphene oxide nanosheets were prepared and added to the PMMA powder (nGOCUR) as previously describe by Khalil and Enaba. [20]

Animals, study design and surgical procedures:

This study was approved by the ethical committee of the Faculty of Dentistry, Ain Shams University (No: FDASU-Rec IR 092307). Four groups of rats (6 animals per group) with total of 24 animals were used for this study and divided as shown in **Table 1**. Sterile surgical technique will apply throughout the experiment. The animals will be anesthetized by intraperitoneal injection with a mixture of ketamine HCl (7 mg/kg) and xylazine (60 mg/kg). The area of implantation will be shaved and sterilized with Betadine at the dorsal side of each animal. A transverse incision of approximately 2.5 cm will be made in the skin with a sterile surgical blade and connective tissue inside were dissected to create a subcutaneous pocket. A section of 2.5 mm of the autoclaved sterile material will be implanted inside the subcutaneous pocket according to the respective groups. The incision will be closed with 5.0 sutures. No implantation was done in sham control animals. Rats were individually caged after surgery and observed for clinical signs and symptoms.

Blood samples:

After 7 days of the surgery and before the sacrifice, animals were bled from the tail vein and 1 ml blood was collected in heparin (2 IU/ml)-containing vial to be used for hematological parameters (CBC) like hemoglobin (Hb; in grams per deciliter), packed cell volume (PCV; in percent), mean corpuscular volume (MCV), total red blood cell (RBC) count, total white blood cell (WBC) count, absolute erythrocyte indices, and differential WBC count.

Histopathological evaluation:

After 1 week (7 days), the rats were sacrificed and the skin part above the implanted scaffolds were harvested and fixed for histopathological examination. A total of 24 specimens were prepared for 4 groups Sham, PMMA, nGO only and nGO with CUR where 6 samples were included per group. We assessed the morphological evaluation of tissue response by light microscope using 5-μm-thick-sections placed onto the glass slides and stained with hematoxylin and eosin (H&E). The tissue block was sectioned with a microtome using a tungsten carbide knife. The counting of Inflammatory cells and thickness of fibrous capsule were determined by a blinded operator to avoid bias.

Mechanical Testing

Flexural strength test

The flexural strength (MPa) of the specimens was evaluated using the 3-point bending test in a universal testing machine (Instron model 3345 England. Data recorded using computer software (Bluehill instron England) with a crosshead speed of 5 mm/min. The 20 specimens (10 in each group) were stored in distilled water at room temperature for 10 days and then retrieved and placed on supporting jigs 40 mm apart. A loading force was applied using a centrally located plunger with a diameter of 20 mm and the maximum load exerted on the specimens until fracture was recorded. The flexural strength was calculated as $F=3PL/2bd^2$, where F is the flexural strength, P is the applied load, L is the support span length, b is the sample width with and d is the sample thickness. The flexural modulus (MPa) was calculated as Ebend=PL3/4Dbd3, where Ebend is the flexural or bending modulus of elasticity equivalent to Young's modulus (E) and D is the deformation. The prepared PMMA modified with nanoparticles displayed higher flexural strength and hardness. Data regarding mechanical properties of the prepared materials has been previously published by our group. [20]

Statistical analysis:

Data were analyzed using Prism software (Graph pad software Inc., San Diego, CA) by one way analysis of variance (ANOVA) with a Newman-Keuls post hoc test. Statistical significance was assigned at $P<0.05$. Data presented in the form of graphs have values representing means ± standard error of the mean (S.E.M).

TABLE (1) Study design

Groups	Description
Sham (negative control) (n=6)	Surgical procedure without an implant
Group A (n=6)	Acrylic only
Group B (n=6)	Acrylic + nGO
Group C (n=6)	Acrylic + nGOCUR

RESULTS

Gross observation of the general condition:

The 24 animals survived the 1-week study period with no signs of mortality or infection. There were no surgery-related or implantation-related abnormalities until the sacrifice.

Blood parameters:

The results of the hematological parameters (white blood cells count, hemoglobin content and red blood cells count) were used to determine implant-associated infections. The value of the sham group (surgery with no implant) was considered the comparative reference. Blood parameters were all within the normal range and not significantly different from the Sham group.

Histological assessment of the tissue surrounding the scaffold:

Immune response to biological materials is a great challenge. Unfavorable immune response interferes with tissue regeneration and repair and leads to injury and/or ulcerations. To validate the biocompatibility and local tissue response, we performed histopathological analysis of the subcutaneous tissue surrounding the implanted materials after 1 week. Histological sections showed normal stratified squamous epithelium with cornified layer, hair follicles, sebaceous glands and bundles of collagen fibers as shown in **Figure 1**. Inflammatory cells were spotted in the surgical sites in all groups. The inflammatory cell count was significantly higher in group A (acrylic) versus the sham group (no implant)**.** However**,** adding nanoparticles of graphene oxide to the acrylic implants (Group B) significantly reduced the inflammatory cell count with a p-value £ 0.0001 **(Table 2 and Figure 3)**. On the other hand, adding CUR to the GO nanoparticles (nGOCUR; Group C) did not reduce the inflammatory cells count as compared to the acrylic only group (Group A).

TABLE (2) Mean and median of inflammatory cells count

Groups	Mean	Median
Sham (negative control)	73	75
Group A (Acrylic)	414	390
Group B Acrylic + Graphene Oxide nanoparticles nGO	282	288
Group C (Acrylic + Graphene Oxide and Curcumin nanoparticles) nGOCUR	409	422

We further measured the thickness of the fibrous tissue capsule surrounding the implanted material. The nGO group significantly reduced the collagen deposition and induced a thinner fibrous capsule surrounding the implanted materials as shown in **Figure 2**.

There was a 4-fold decrease in the fibrous tissue capsule in the nGO group as compared to the PMMA group. Surprisingly, adding curcumin to the nGO nanoparticles (nGOCUR group), though did not reduce the inflammatory cell count, it did attenuate the thickening of the fibrous capsule surrounding the implant as shown in **Table 3**. This post-necropsy histopathological examination of the skin surrounding the implanted scaffold rules out any associated infections or adverse systemic effects of the tested material.

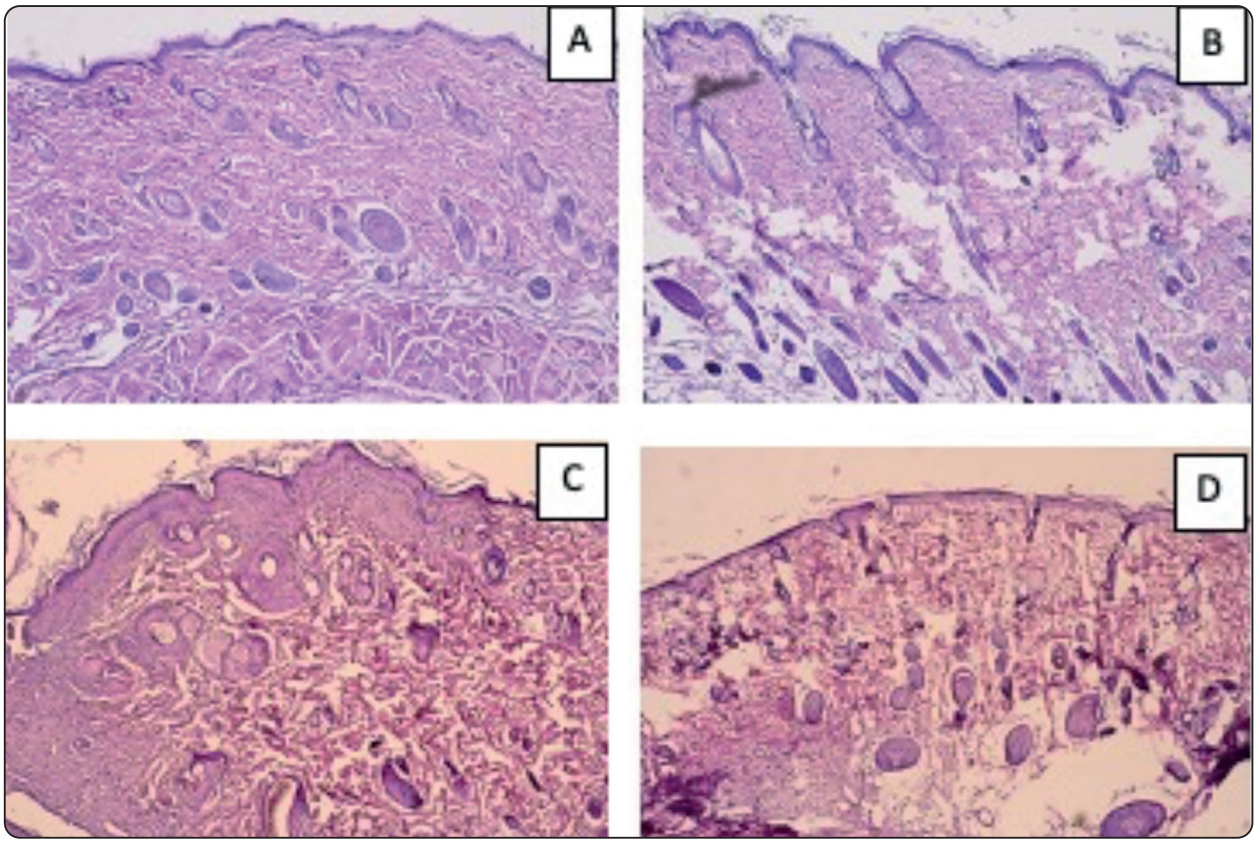

Fig. (1) H&E skin sections of the different groups showing normal skin morphology. (A) Sham, (B) Acrylic, (C) Acrylic + GO, (D) Acrylic + GO + Curcumin (x10)

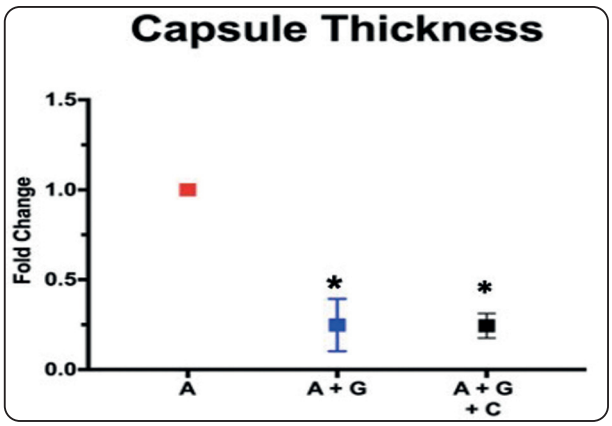

Fig. (2) Measurement of the granulation tissue thickness (capsule thickness). Measurements are expressed as fold change compared to the acrylic group. A: acrylic group, A+G: Acrylic and GO nanoparticles, A+G+C: Acrylic, GO nanoparticles and curcumin. * Compared to acrylic group

TABLE (3) Mean and median thickness of the fibrous capsule surrounding the implanted material

Groups	Mean	Median
Group A (Acrylic)	446	413
Group B (Acrylic + Graphene Oxide nanoparticles) nGO	110	94
Group C (Acrylic + Graphene Oxide and Curcumin nanoparticles) nGOCU	108	102

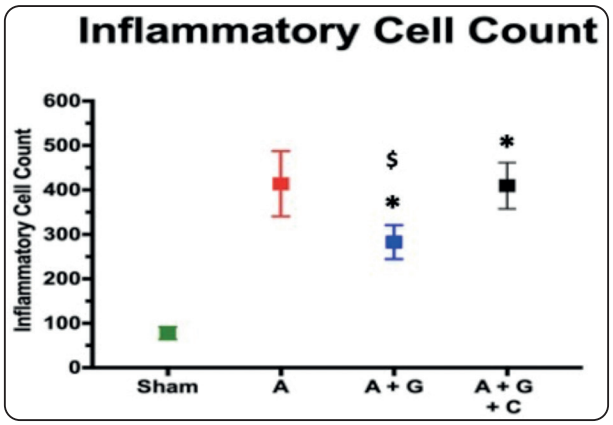

Fig. (3) Inflammatory cells count of H & E-stained histological sections of the skin surrounding the defect in different experimental groups (sacrificed 10 after days after the surgical procedures). *p £ 0.0001 (* compared to Sham), ($ compared to Acrylic only)

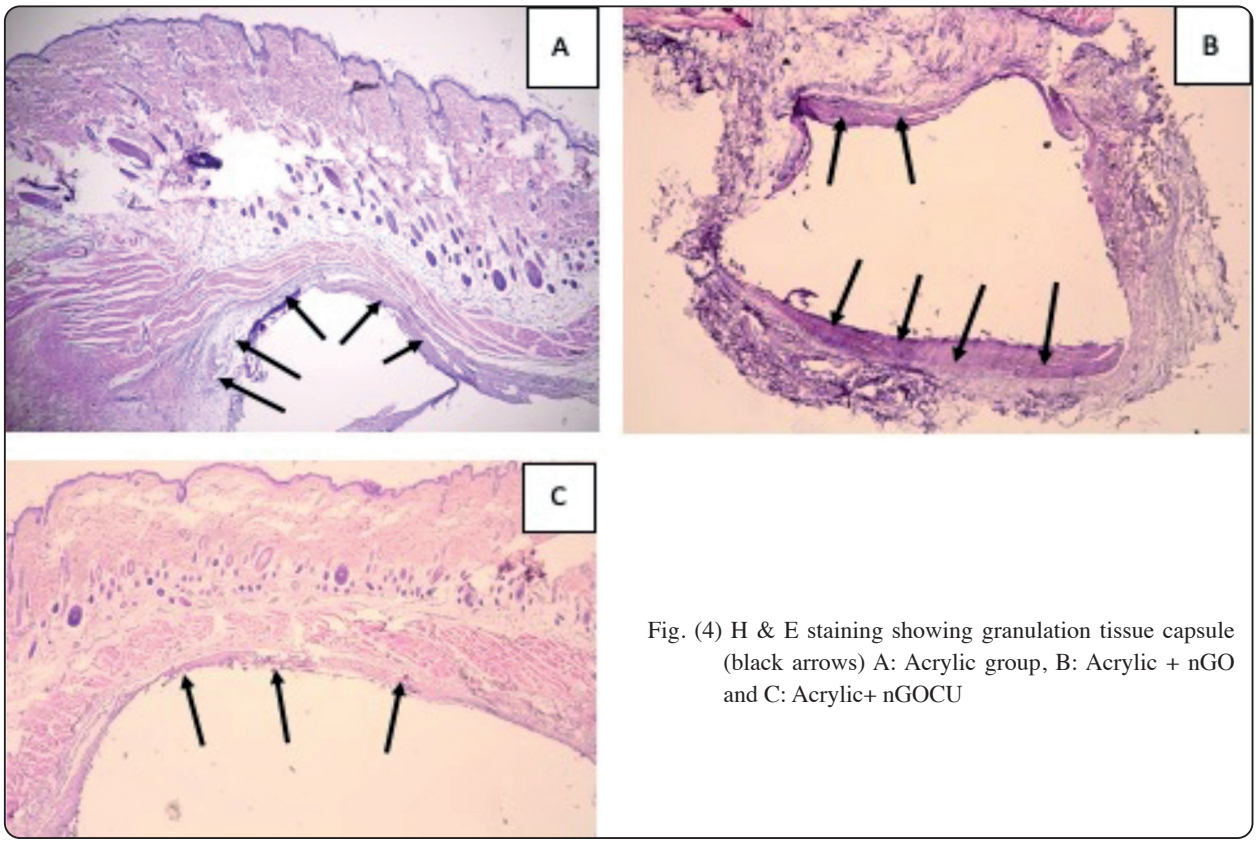

Fig. (4) H & E staining showing granulation tissue capsule (black arrows) A: Acrylic group, B: Acrylic + nGO and C: Acrylic+ nGOCU

DISCUSSION

In this study, we are examining the *in vivo* biocompatibility of PMMA impregnated with GO nanoparticles with or without CUR. We evaluated the biocompatibility of these materials by subcutaneous implantation of 5-mm acrylic samples impregnated with the selectively prepared nanoparticles (nGO only and nGOCUR) in a Wistar rats. In accordance with previous studies, the animals did not show any signs of cytotoxicity or local infection and normal skin architecture was observed. As expected, mild immunological response presented as inflammatory cells infiltration was observed in the H and E-stained tissue of all specimens. Immunological response was maximum in the animals having acrylic samples without nanoparticles and minimum in the sham group. Although all animals implanted with the different acrylic specimens showed higher inflammation than the sham group, the nGO group

revealed significantly less degree of inflammation as compared to the PMMA group. On the other hand, the nGOCUR group showed a slight decrease in the inflammatory cells count that was insignificant as compared to the PMMA group. This major decrease in the inflammatory reaction in the nGO group was marked by the regression of the inflammatory cell count as shown in **Figure 3**.

These results are in accordance with other *In vitro* biocompatibility studies of nGO loaded with other materials and its favorable effect in lowering local inflammation. [5,17] Since the formation of granulation tissue is a crucial step in assessing post-surgical healing, we measured the thickness of the granulation fibrous tissue capsule formed in the implantation sites. As expected, granulation tissue capsules, representing a normal stage of the healing process, were detected in all the specimens having implanted materials. The capsule thickness was reduced more than 50% in the nGO and nGOCUR groups as compared to PMMA only. This reduction was statistically significant in both groups.

Biocompatibility is a key feature for a successful biomaterial. In biomedical applications, a functional material should not be toxic or immunogenic to living tissues. Though, the skin structure, immunological reactions and wound-healing mechanisms in rodents are different from humans which is a limitation of animal models, using rat models is still a useful research tool for pre-clinical studies. The *in vivo* biocompatibility of a material can be evaluated by subcutaneous or intramuscular implantation using a rat model. This strategy has been repeatedly used in multiple dental and medical studies. [21–23] For example, Jaiswal et al. have examined the biocompatibility of gel and hydroxyapatite poly-L-lactic acid scaffolds and compared their local and systemic effects in a rat model. [21] Another recent study by Samat et al. examined the In vivo biocompatibility of a 3D-printed thermoplastic scaffold of polyurethane/polylactic acid blend by subcutaneous surgical insertion in a rat model. [24]

Healing is a physiologically complex phenomenon that involves sequential processes of inflammation, proliferation and remodeling phases. [25] After injury, a cascade of inflammation follows with the release of chemokines and growth factors that eventually achieve successful homeostasis. The proliferative phase following inflammation and granulation tissue starts forming 2-4 days after injury. Around 10 days after injury, it shifts to the remodeling and re-organization phase. [26,27] Approximately after 7 days, epithelium regenerate to cover the wound and highly vascular granulation tissue forms in the dermis around the implanted specimens [25,26].

All our specimens showed a distinct layer of granulation tissue which is an expected and normal response of the healing process. Subcutaneous placement of acrylic samples impregnated with graphene nanoparticles resulted in a well-formed thinner granulation tissue capsule as compared to the acrylic alone. Impregnating the acrylic graphene oxide samples with curcumin improved the tissue response as compared to the acrylic alone, but was not different from the acrylic and nGO samples. A thinner granulation tissue capsule around a synthetic subcutaneously implanted material is sign of favorable tissue response and hence adding nGO to acrylic improves its biocompatibility. [28]

Using nanotechnology in improving the properties of PMMA is an interesting point of research especially with its increased dental and non-dental uses.[29,30] This improvement can employ several advantages such as better physicochemical, immune compatibility and anti-microbial properties. [31,32]

Several studies have focused on the physical properties of PMMA/GO orthopedic cements. [16,33] A study by Paz et al. in 2019 has verified that incorporating powder of GO nanoparticles did not significantly affect its polymerization nor its thermal properties. [34] Furthermore, this group has confirmed the *In vitro* biocompatibility and lack of cytotoxic effects of the tested powder on pre-osteoblasts

(MC3T3) after 72 hours of incubation. This study has not observed an anti-microbial effect for the incorporated nGO to PMMA, however, other studies have reported an anti-microbial effect for nGO. [8,35,36] The conflict between different studies can be attributed to time-dependent bactericidal effect of GO that involves regulatory proteins related to the generation of intracellular oxidative stress and disruption of the bacterial cell membrane. [37]

Combining the use of curcumin and GO nanoparticles have been previously investigated. This combination achieved better antibacterial properties and also improved the pro-proliferative and attachment properties of NIH3/T3 fibroblasts. (38) The bactericidal effect of GO/curcumin combination has been repeatedly verified. [39] In our study, we assessed the anti-inflammatory and pro-healing effect of adding curcumin and GO to PMMA. As shown, adding curcumin was useful in the healing improvement, however, the effect was not significantly superior to the GO.

In conclusion, incorporating GO nanoparticles to PMMA did not exhibit any cytotoxicity as shown by the general well-being and normal hematologic counts of the tested animals. The tissues surrounding the subcutaneous inserts displayed reduced number of inflammatory cells and thinner granulation tissue capsule after 7 days of inserting the PMMA/nGO. Adding nCUR particles also significantly reduced the capsule thickness, but had insignificant effect on the inflammatory cells count. Adding nGO nanoparticles to PMMA had no negative effect on the overall mechanical properties of the material.

Funding declaration statement: I would like to declare this the paper was not supported by any sponsor or funder.

REFERENCES

1. Priyadarsini S, Mukherjee S, Mishra M. Nanoparticles used in dentistry : A review. J Oral Biol Craniofacial Res [Internet]. 2018;8(1):58–67. Available from: http://dx.doi.org/10.1016/j.jobcr.2017.12.004
2. Barot T, Rawtani D, Kulkarni P. Nanotechnology-based materials as emerging trends for dental applications. Rev Adv Mater Sci. 2021;60(1):173–89.
3. Ren J, Braileanu G, Gorgojo P, Valles C, Dickinson A, Vijayaraghavan A, et al. On the biocompatibility of graphene oxide towards vascular smooth muscle cells. Nanotechnology. 2020;32(5).
4. Singh S, Hasan MR, Sharma P, Narang J. Graphene nanomaterials : The wondering material from synthesis to applications. Sensors Int [Internet]. 2022;3(June):100190. Available from: https://doi.org/10.1016/j.sintl.2022.100190
5. Elkhenany H, Amelse L, Lafont A, Bourdo S, Caldwell M, Neilsen N, et al. Graphene supports in vitro proliferation and osteogenic differentiation of goat adult mesenchymal stem cells: Potential for bone tissue engineering. J Appl Toxicol. 2015;35(4):367–74.
6. Mancinelli R, Di Filippo ES, Tumedei M, Marrone M, Fontana A, Ettorre V, et al. Human dental pulp stem cell osteogenic differentiation seeded on equine bone block with graphene and melatonin. Appl Sci. 2021;11(7).
7. Di Crescenzo A, Zara S, Di Nisio C, Ettorre V, Ventrella A, Zavan B, et al. Graphene Oxide Foils as an Osteoinductive Stem Cell Substrate. ACS Appl bio Mater [Internet]. 2019;2(4):1643–51. Available from: http://europepmc.org/abstract/MED/35026898
8. Di Giulio M, Di Lodovico S, Fontana A, Traini T, Di Campli E, Pilato S, et al. Graphene Oxide affects Staphylococcus aureus and Pseudomonas aeruginosa dual species biofilm in Lubbock Chronic Wound Biofilm model. Sci Rep. 2020;10(1):1–9.
9. Li M, Xiong P, Yan F, Li S, Ren C, Yin Z, et al. An overview of graphene-based hydroxyapatite composites for orthopedic applications. Bioact Mater. 2018 Jan 30;3.
10. Amiryaghoubi N, Noroozi Pesyan N, Fathi M, Omidi Y. Injectable thermosensitive hybrid hydrogel containing graphene oxide and chitosan as dental pulp stem cells scaffold for bone tissue engineering. Int J Biol Macromol [Internet]. 2020;162:1338–57. Available from: https://www.sciencedirect.com/science/article/pii/S0141813020335790
11. Jaworski S, Hinzmann M, Sawosz E, Grodzik M, Kutwin M, Wierzbicki M, et al. Interaction of different forms of graphene with chicken embryo red blood cells. Environ Sci Pollut Res. 2017;24(27):21671–9.

12. Liao K-H, Lin Y-S, Macosko CW, Haynes CL. Cytotoxicity of Graphene Oxide and Graphene in Human Erythrocytes and Skin Fibroblasts. ACS Appl Mater Interfaces [Internet]. 2011 Jul 27;3(7):2607–15. Available from: https://doi.org/10.1021/am200428v

13. Vallabani NVS, Mittal S, Shukla RK, Pandey AK, Dhakate SR, Pasricha R, et al. Toxicity of graphene in normal human lung cells (BEAS-2B). J Biomed Nanotechnol. 2011 Feb;7(1):106–7.

14. Pelin M, Fusco L, Martín C, Sosa S, Frontiñán-rubio J, González-domínguez JM. Nanoscale Graphene and graphene oxide induce ROS production in human HaCaT skin keratinocytes : the role of xanthine oxidase and NADH. 2018;11820–30.

15. Oxide G, Epithelial L, Bengtson S, Kling K, Madsen AM, Noergaard AW, et al. No Cytotoxicity or Genotoxicity of Graphene and. 2016;482(May).

16. Hung HS, Kung ML, Chen FC, Ke YC, Shen CC, Yang YC, et al. Nanogold-carried graphene oxide: Anti-inflammation and increased differentiation capacity of mesenchymal stem cells. Nanomaterials. 2021;11(8).

17. Hoyle C, Rivers-auty J, Vranic S, Wang E, Buggio M, Rothwell NJ, et al. Small, Thin Graphene Oxide Is Anti-infl ammatory Activating Nuclear Factor Erythroid 2 - Related Factor 2 via Metabolic Reprogramming. 2018;

18. Gautam R, Singh RD, Sharma VP, Siddhartha R, Chand P, Kumar R. Biocompatibility of polymethylmethacrylate resins used in dentistry. J Biomed Mater Res - Part B Appl Biomater. 2012;100 B(5):1444–50.

19. Zebarjad SM, Sajjadi SA, Sdrabadi TE. A Study on Mechanical Properties of PMMA / Hydroxyapatite Nanocomposite. 2011;2011(August):795–801.

20. Khalil M, Enaba L. Influence of Antimicrobial Nanoparticles on Flexural Strength and Hardness of Polymethylmethacrylate. 2021;9(D):314–8.

21. Jaiswal AK, Dhumal R V., Bellare JR, Vanage GR. In vivo biocompatibility evaluation of electrospun composite scaffolds by subcutaneous implantation in rat. Drug Deliv Transl Res. 2013;3(6):504–17.

22. Modulevsky DJ, Cuerrier CM, Pelling AE. Biocompatibility of Subcutaneously Implanted Plant-Derived Cellulose Biomaterials. PLoS One. 2016;11(6):1–19.

23. Priya G, Madhan B, Narendrakumar U, Suresh Kumar RV, Manjubala I. In Vitro and in Vivo Evaluation of Carboxymethyl Cellulose Scaffolds for Bone Tissue Engineering Applications. ACS Omega. 2021;6(2):1246–53.

24. Abdul Samat A, Abdul Hamid ZA, Jaafar M, Ong CC, Yahaya BH. Investigation of the In Vitro and In Vivo Biocompatibility of a Three-Dimensional Printed Thermoplastic Polyurethane/Polylactic Acid Blend for the Development of Tracheal Scaffolds. Bioengineering. 2023;10(4).

25. Wang P, Huang B, Horng H, Yeh C. Wound healing. J Chinese Med Assoc [Internet]. 2018;81(2):94–101. Available from: https://doi.org/10.1016/j.jcma.2017.11.002

26. Häkkinen L, Larjava H, Koivisto L. Granulation tissue formation and remodeling. 2012;94–129.

27. Gauglitz GG, Korting HC, Pavicic T, Ruzicka T, Jeschke MG. Hypertrophic scarring and keloids: Pathomechanisms and current and emerging treatment strategies. Mol Med. 2011;17(1–2):113–25.

28. Elreash AA, Hamama H, Abdo W, Wu Q, El-din AZ, Xiaoli X. Biocompatibility of new bioactive resin composite versus calcium silicate cements : an animal study. 2019;1–10.

29. Li X, Liang X, Wang Y, Wang D, Teng M, Xu H. Graphene-Based Nanomaterials for Dental Applications : Principle, Current Advances, and Future Outlook. 2022; 10(March):1–21.

30. Priyadarsini S, Mohanty S, Mukherjee S, Basu S, Mishra M. Graphene and graphene oxide as nanomaterials for medicine and biology application. J Nanostructure Chem [Internet]. 2018;8(2):123–37. Available from: https://doi.org/10.1007/s40097-018-0265-6

31. de Castro DT, Valente MLC, Agnelli JAM, Lovato da Silva CH, Watanabe E, Siqueira RL, et al. In vitro study of the antibacterial properties and impact strength of dental acrylic resins modified with a nanomaterial. J Prosthet Dent [Internet]. 2016;115(2):238–46. Available from: https://www.sciencedirect.com/science/article/pii/S0022391315005065

32. Vojdani M, Giti R. Polyamide as a Denture Base Material: A Literature Review. J Dent (Shiraz, Iran) [Internet]. 2015 Mar;16(1 Suppl):1–9. Available from: https://pubmed.ncbi.nlm.nih.gov/26106628

33. Soleymani S, Bakhtiari E, Bakhsheshi-rad HR, Karbasi S, Ramakrishna S, Berto F. Polymethyl Methacrylate-Based Bone Cements Containing Carbon Nano-tubes and Graphe Oxide: An overview of Physicla, Mechanical and Biological Properties. Polymers (Basel). 2020;12(7).

34. Paz E, Ballesteros Y, Abenojar J, del Real JC, Dunne NJ. Graphene Oxide and Graphene Reinforced PMMA Bone Cements: Evaluation of Thermal Properties and Biocompatibility. Vol. 12, Materials. 2019.

35. Saeed SI, Vivian L, Zalati CWSCW, Izreen N, Sani M, Aklilu E. Antimicrobial activities of graphene oxide against biofilm and intracellular Staphylococcus aureus isolated from bovine mastitis. BMC Vet Res [Internet]. 2023;1–11. Available from: https://doi.org/10.1186/s12917-022-03560-6

36. Kim H, Cho H, Whitney U. Direct-Deposited Graphene Oxide on Dental Implants for Antimicrobial Activities and Osteogenesis. 2021;(July).

37. Ravikumar V, Mijakovic I PS. Antimicrobial Activity of Graphene Oxide Contributes to Alteration of Key Stress-Related and Membrane Bound Proteins. Int J Nanomedicine. 2022;28(17):6707–21.

38. Nowroozi N, Faraji S, Nouralishahi A, Shahrousvand M. Biological and structural properties of graphene oxide / curcumin nanocomposite incorporated chitosan as a scaffold for wound healing application. 2021;264(October 2020).

39. Cacaci M, Squitieri D, Palmieri V, Torelli R, Perini G, Campolo M, et al. Curcumin-Functionalized Graphene Oxide Strongly Prevents Candida parapsilosis Adhesion and Biofilm Formation. 2023;1–17.